

B.R.Ilyassov^{1,2}, N.Kh.Ibrayev¹

¹*Institute of Molecular Nanophotonics, Ye.A.Buketov Karaganda State University;*

²*Laboratory of Solar Energy, PINLA, Nazarbayev University, Astana
(E-mail: baurzhan.ilyassov@nu.edu.kz)*

Recent achievements in perovskite solar cells

Hybrid (organo-inorganic) perovskite materials are potential candidate as a photoactive materials for photovoltaics. Currently, many research groups have been focused on designing the perovskite materials in such a way so that it can harness the broad spectrum of visible light wavelength. Hybrid perovskites such methylammonium lead halides reveal unique photovoltaic and charge transport properties. The main objectives of this article are to provide some recent research progress on perovskite nanomaterials for solar cell application. Therefore, this mini review paper summarizes some recent development of organic-inorganic perovskite materials of different research groups and provides some useful insights for its future improvement.

Key words: photoactive materials, photovoltaics, hybrid perovskites, nanomaterials, sunny batteries.

Introduction

The world's growing population and industrialization result in a constantly rising demand for energy. Uses of fossil fuels as an energy source produce greenhouse gases which have detrimental effect on the environment, especially global warming [1–3]. Are we willing to accept the effect of greenhouse gases on climate change in order to meet our energy demand? If we are not we need to urgently solve the challenging problem of developing alternative sources of energy that can make a difference. Harnessing energy directly from sunlight can be an alternative approach to fulfil the clean energy need with negligible environmental effect. Developing of photovoltaic (PV) and water splitting devices based on the remarkable perovskite materials are one of the important step toward achieving that goal.

Organic-lead halide perovskites have the potential to be such an alternative technology for energy production. Power conversion efficiencies (PCE) of PV devices based on these materials have increased from around 4 % to a certified 20.1 % in the last three years [4–7]. Due to their high efficiency, perovskite solar cells are already competing established thin-film technologies, such as those based on inorganic semiconductor CdTe and CIGS [8]. These organic-lead halide perovskites show high photon absorptivity in optical range, and a sharp optical band edge, which suggests low levels of disorder.[9, 10] They also exhibit long charge-carrier diffusion lengths (>1 μm) relative to the absorption depth of incident light (~100 nm) [11–14], meaning that almost all photoexcited charge carrier in the perovskite are able to reach the interfaces from where the charges are then transported through suitable hole and electron-transporting layers to the electrodes.

Despite progress in the efficiency of PCSs, there is still challenges to commercialization because of the toxicity of Pb atoms, longterm stability, and (3) cost-effectiveness. We have extremely large field for researching to improve and optimize perovskite solar cells in order to soon as possible see these remarkable solar cells on the market.

In this review paper, it is intended to provide the recent progress in perovskites for the application in photovoltaics. In the first section, we introduce the perovskite structure. In Section 2, recent progress in organolead halide perovskite, deposition processes of organolead perovskite for solar cells and the operation principles of perovskite solar cells are discussed. Finally, in Section 3, some conclusions are drawn on future perspective of perovskite materials.

1. The structure of perovskites materials

Perovskite materials have similar crystal structures to calcium titanate (CaTiO₃). The compounds with perovskite structure exist widely in earth, and some researchers believe that magnesium silicate perovskite (MgSiO₃) is the most prevalent mineral in the mantle of the earth [15]. Perovskite materials have various interesting properties and practical applications such as large magnetoresistance, superconductivity, ferroelectricity, transport properties, optical properties, etc. which can be utilized in designing effective devices for photovoltaic and photocatalysts for water splitting. The perovskite structure can be expressed

by generalized formula of ABX_3 , where the B atom is usually a metal cation and X is an anion (O^{2-} , I^- , Br^- , Cl^- , etc.) [16]. They form the BX_6 octahedral where X lies in the corner around B located at the center of the octahedral (Figure 1a). The BX_6 octahedral form an extended three dimensional space network with all-corner connected each other (Fig. 1b). The symbol A is assigned to a metal cation that fills the vacancy among the octahedral and balances the charge of the whole network. The larger A cations (Ca^{2+} , K^+ , Na^+ , Sr^{2+} , Pb^{2+} , Ce^{3+}) occupy the 12 coordinated sites between the octahedral. In the idealized cubic unit cell, the position of cation A sites, cation B sites and anion X sites are at cube corner positions (0,0,0), body center position (1/2,1/2,1/2) and face centered positions (1/2,1/2,0), respectively. The examples of ideal cubic perovskite structure (undistorted cubic structure) are $SrTiO_3$ [17], $CsSnBr_3$ [18].

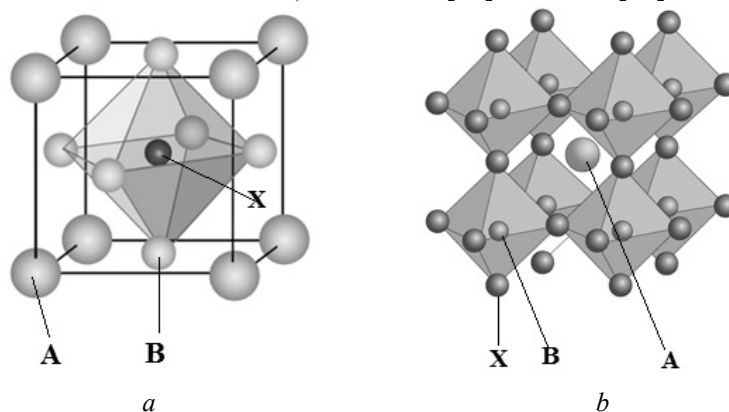


Figure 1. ABX_3 perovskite structure showing BX_6 octahedral geometry (a) and their extended network structure connected by the corner-shared octahedral (b). Reprinted from [15] and [19]

In most cases, the perovskites have distorted type of cubic structure. These distortions are enormous in number and have complex details. Even the $CaTiO_3$ mineral has pseudo-cubic structure due to the tilting of the octahedron. According to Ziyong Cheng and Jun Lin [16] the various distortion mechanisms can be classified into five types: (1) distortion of the BX_6 octahedron by the Jahn-Teller effect, (2) off-center displacement of the B cations in the BX_6 octahedron, this effect is responsible for possible ferroelectricity, (3) so-called tilting of the octahedra framework, typically occurring as result of a too small A cation at the cuboctahedral site, (4) ordering of more than one kind of cations A or B, or of vacancies, (5) ordering of more than one kind of anions X, or vacancies. Physical properties of perovskite materials depend crucially on these distortions, particularly the electronic, optical, transport, magnetic and dielectric properties which are significant for many applications of perovskite materials. Therefore, the distortions as a result of cation substitution can be used for tuning physical properties exhibited by perovskites.

2.1 Recent progress in organolead halide perovskite for solar energy conversation

The prevalent perovskite materials used in solar cells to date are three-dimensional hybrid perovskites. These perovskites have short-chain organic cations, such as methylammonium ($CH_3NH_3^+$, MA), metal cations such as lead (Pb^{2+}), and halides ($X = I^-$, Br^- , Cl^- or mixtures). For efficient devices, cation B has been Pb^{2+} . Although, Sn^{2+} forms similar structure with lower and naturally more ideal bandgaps [20], but with lower stability. In this Section, we will focus on the $MAPbI_3$ and the mixed-halide analogue, $MAPbI_{3-x}Cl_x$ perovskite films. We will present a recent progress in organolead halide perovskite, the different methods for the formation of films and consider the operation principles of perovskite solar cells which are not fully understood yet.

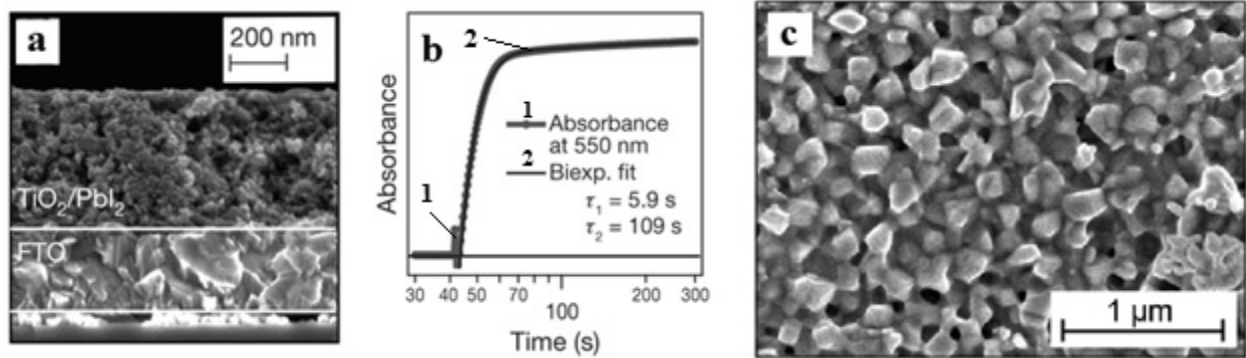
In 2013, one of Science's Top 10 Breakthroughs of 2013 has become highly efficient organolead halide perovskite solar cells [21]. In perovskite solar cell (PSCs), the organolead halide perovskite, $CH_3NH_3PbX_3$ (where $X = I^-$, Br^- , Cl^-), is used as a photoactive layer to harvest sunlight. In 2009, Miyasaka et al. first published a report on using perovskite nanoparticles as visible light sensitizers in liquid DSSC based on mesoporous TiO_2 scaffold yielding efficiencies of 3.81 % [22]. However, these first DSSCs sensitized by perovskite nanoparticles had poor stability because of liquid electrolyte which corrupts perovskite sensitizer. In 2009, Grätzel's group also used the perovskite nanoparticles to sensitize mesoporous TiO_2 films in a solid-state mesoscopic solar cell and delivered power conversion efficiency (PCE) of up to 9.7 % [23]. They used hole-conductor spiro-MeOTAD instead of liquid electrolyte. Soon, Snaith's group employed mesoporous Al_2O_3 as a scaffold and a mixed halide perovskite, $CH_3NH_3PbI_{3-x}Cl_x$, as sunlight absorber.

The insulating Al_2O_3 scaffold supports the formation of continuous thin films of $\text{CH}_3\text{NH}_3\text{PbI}_{3-x}\text{Cl}_x$ and extremely decreases the energy costs associated with separating tightly bound excitons (photoinduced electron-hole pairs) and extracting free charges from highly disordered low-mobility networks such as mesoporous TiO_2 . That so-called «meso-superstructure» PCS had a PCE as high as 10.9 % and generated open-circuit photovoltage of more than 1.1 volts [24]. This study for the first time demonstrated that the mixed halide perovskite could be as both a sunlight absorber and a charge carrier transporter. The PCE of the perovskite solar cell was further increased up to 12 % by the infiltrating the pores of the mesoporous TiO_2 film with $\text{CH}_3\text{NH}_3\text{PbI}_3$ perovskite, and overlayers of $\text{CH}_3\text{NH}_3\text{PbI}_3$ co-exist on top of the mp- TiO_2 film [25]. This study implied that the perovskite performs a double role as light harvester and hole conductor. A significant improvement in the PCSs fabrication and reproducibility of their performance was achieved introducing a two-step sequential deposition technique. PbI_2 was first introduced from solution into an mp- TiO_2 film and subsequently transformed into the perovskite by exposing it to a solution of $\text{CH}_3\text{NH}_3\text{I}$, resulting in a cell with a PCE of 15 % [26]. Further, Snaith's group showed that nanostructuring is not necessary to achieve high efficiencies with this material [27]. They obtained PCE of 15 % in simple planar heterojunction solar cell incorporating vapour-deposited perovskite as the absorbing layer, a compact layer of n-type TiO_2 as an electron-collecting layer, and spiro-MeOTAD as a p-type hole conductor. This study demonstrated that perovskite absorbers can function with the highest efficiencies in simplified device architectures, without the need for complex nanostructures. Y. Yang et al. reported a planar PSC with a PCE of 19.3 % using the efficient interface engineering technology. By controlling the formation of the perovskite layer and careful choices of other materials, they suppressed carrier recombination in the absorber, facilitated carrier injection into the carrier transport layers, and maintained good carrier extraction at the electrodes [28]. Recently, the certified PCE of PSC has been boosted up to 20 % [29], which is the most promising competitor to silicon-based solar cells.

2.2. Deposition processes of organolead perovskite for solar cells

In the first reports on $\text{CH}_3\text{NH}_3\text{PbI}_3$ and $\text{CH}_3\text{NH}_3\text{PbI}_{3-x}\text{Cl}_x$ solar cells, spin-coating technique was used to prepare the photoactive absorbers from a single precursor solution. A solution of $\text{CH}_3\text{NH}_3\text{I}$ and PbI_2 (stoichiometric ratio) in polar solvents such as GBL or DMF was used to form $\text{CH}_3\text{NH}_3\text{PbI}_3$ films [7, 25]. For forming $\text{CH}_3\text{NH}_3\text{PbI}_{3-x}\text{Cl}_x$, a solution of PbCl_2 and $\text{CH}_3\text{NH}_3\text{I}$ (a molar ratio of 1:3) in DMF was usually used [30, 31]. The perovskite absorber can be deposited either within the pores of the mesoporous layers or be formed as uniform films on TiO_2 compact layers in a case of planar solar cells by proper optimization of the precursor concentration and spin-coating conditions. For planar cells, the deposition of a uniform perovskite layer by spin-coating demand the optimization of various parameters including post-deposition treatment [32, 33]. Since wettability of underlying layer is different, the deposition of perovskite must need to be separately optimized for each of ones. The degree of infiltration within the mesoporous layer depends crucially upon the solution concentration, spin-coating rate and the properties of solvent used. The roughness of surface which could cause shunts in the solar cells depends on the tendency perovskite films to crystallize [25].

An important achievement in solution based deposition has been the development of the sequential deposition method for the preparation of perovskite solar cells by Grätzel and coworkers [26]. These deposition method is composed of spin-coating PbI_2 layer on the TiO_2 mesoporous layer from a solution under proper conditions (solution concentration, spin-coating rate) that allow to qualitatively infiltrate PbI_2 within the mesoporous layer (first step) (Fig. 2a). Subsequently, the substrates with formed PbI_2 which has yellow color are dipped in a $\text{CH}_3\text{NH}_3\text{I}$ solution in 2-propanol solvent. Over the dipping, the yellow PbI_2 layer converts forming the dark brown $\text{CH}_3\text{NH}_3\text{PbI}_3$ that occurs in a few seconds (Fig. 2b). It is worth to mentioning that the conversion time can depends on different PbI_2 deposition conditions. It has been reported on a 20 minute conversion time [34], though the original work by Mitzi and co. informed that the conversion took 1–3 h [35]. It is probable that the PbI_2 layer deposited on top of mesoporous layers has increased roughness that promotes the conversion reaction [26]. The conversion of PbI_2 into $\text{CH}_3\text{NH}_3\text{PbI}_3$ occurs with volume expansion [36] (~75 %) therefore it is believed that the mesoporous layer would be better infiltrated by the sequential deposition process. The SEM top view of samples deposited by this process show a highly crystalline film with complete coverage (Fig. 2c).



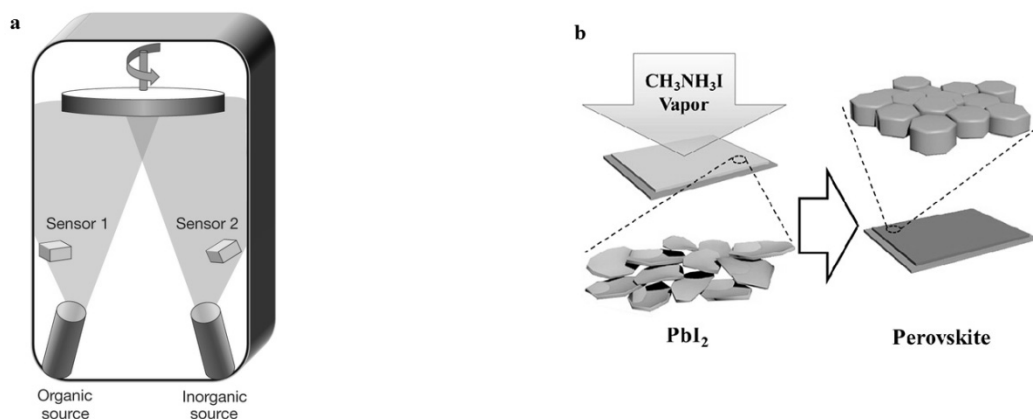
Cross-sectional SEM image of a mesoporous TiO_2 film infiltrated with PbI_2

Changing in absorbance at 550 nm of such a film monitored during the conversion from PbI_2 to $\text{CH}_3\text{NH}_3\text{PbI}_3$

SEM top view of the $\text{CH}_3\text{NH}_3\text{PbI}_3$ film prepared utilizing the sequential deposition method

Figure 2. Reprinted from [26]

Vapour deposition techniques have also been used to form perovskite solar cells along with the extensively applied solution based deposition processes. Efficient planar solar cells (15.4 %) of $\text{CH}_3\text{NH}_3\text{PbI}_{3-x}\text{Cl}_x$ fabricated by dual source evaporation of PbCl_2 and $\text{CH}_3\text{NH}_3\text{I}$ (Figure 3a) were showed by Snaith and coworkers [27]. The evaporated perovskite film was sandwiched between a compact TiO_2 layer and a spin-coated spiro-OMeTAD layer performing as electron and hole transporters, respectively. The vapour-deposited perovskite films are extremely uniform and compact, with crystal grains of hundreds of nanometers. By these vapour deposition technique, Bolink and coworkers [37] managed to fabricate device with efficiency 12.04 % utilizing different electron and hole transporters, organic electron and hole transport layers such as PCBM and PEDOT: PSS. In both cases, in order to yield the desired perovskite layers and efficient solar cells, careful optimization of dual source evaporation process was required. Chen et al. has demonstrated a combined approach in which both solutions based deposition and vapour phase transformation has been utilized [36]. In these so called vapour-assisted solution process (VASP), PbI_2 solution was first spin-coated on a compact TiO_2 substrate. Subsequently, the yellow colored films underwent a vapour of $\text{CH}_3\text{NH}_3\text{I}$ at 150 °C in N_2 for 2 h (Fig. 3b). Due to the slow rate of conversion, VASP produced $\text{CH}_3\text{NH}_3\text{PbI}_3$ films with micron sized grains and with very low surface roughness of ~ 20 nm. Perovskite solar cells fabricated from such films had an efficiency of 12.1 %.



A schematic illustration of dual-source thermal evaporation equipment for depositing the perovskite films; the organic source was methylammonium iodide and the inorganic source PbCl_2 . Reproduced from [27]

A schematic illustration of the vapour assisted conversion of PbI_2 to $\text{CH}_3\text{NH}_3\text{PbI}_3$ by exposure to $\text{CH}_3\text{NH}_3\text{I}$ vapour. Reproduced from [36]

Figure 3

2.3. The operation principles of perovskite solar cells

As mentioned above the perovskite nanoparticles were first used as 'sensitizers' on mesoporous TiO_2 and their role in the solar cell was supposed to be similar to the dye in a DSSC. Sunlight is absorbed by the perovskite nanoparticles, producing electrons in the conduction band of the TiO_2 , across which electrons are transported to the anode. The holes remaining on the perovskite bulk are then transferred to a redox electrolyte, or solid-state hole-transport materials, and further transported to a cathode [38] (Fig. 4a). Further studies revealed that the perovskites can function as both hole and electron transport material [5, 39], and that a thin perovskite film with a thickness of few hundred nanometer can even perform charge generation and transport [5, 31, 40–42]. The cell architectures are similar to a planar heterojunction architecture, where a perovskite layer is sandwiched between *p*- and *n*-type selective contacts [27] (Fig. 4b). This simple planar architecture can be assembled by different preparation methods and strongly attracted attention of photovoltaic [30–60].]

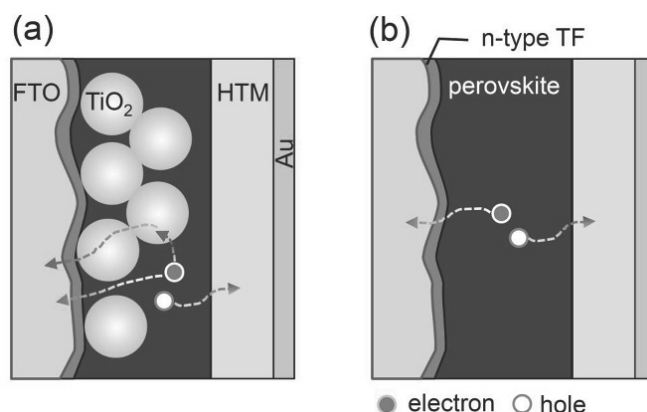


Figure 4. (a) Mesoscopic perovskite solar cell with mesoporous TiO_2 layer and (b) planar structure without a mesoporous TiO_2 layer. Thin film on fluorine doped tin oxide (FTO) is an *n*-type semiconductor. HTM stands for hole transporting material. In the mesoscopic structure, electrons can be collected directly and/or via TiO_2 layer

In planar perovskite solar cells, the charge generation mechanism and dynamics are not completely clear yet. It is not understood what is photoexcited species, free electrons and holes or bound excitons? In the room-temperature, the upper bound of exciton binding energy in the perovskite materials with tetragonal phase is ~ 50 meV [43]. However, in these computation dielectric constant is supposed to be 6.5, but according to Even J. et al., the effective dielectric constant is probable much greater. In that case, exciton binding energies in the tetragonal phase is probable ~ 1 – 10 meV [44]. Though, even for the exciton binding energy of ~ 50 meV, free charge carriers are generated spontaneously after light harvesting, that controversial to a large concentration of bound excitons [43–46]. According to ultrafast spectroscopy studies (Fig. 5a), dissociation of exciton occur during 2 ps after photoexcitation [48, 49]. For confirmation of these features it is required thorough interpretation of these transient spectra. The mobilities of free electrons and holes are approximately equal and lay in the range ~ 10 – 30 $\text{cm}^2 \text{V}^{-1} \text{s}^{-1}$ [49–51] (Fig. 5a inset). Stranks S.D. et al. studied recombination kinetics in organic-inorganic perovskites under high light intensities, according to them; recombination is bimolecular [46]. This indicates that the prevalent relaxation pathway is recombination of free electrons and holes [48, 52]. The recombination in these perovskite is mainly radiative as well. At room temperature, photoluminescence quantum efficiencies reach value of 70 % (Fig. 5b) [46, 48] and at low temperature even 100 % [58]. This high luminescence efficiency ascribes perovskite solar cells to the efficiency limit Shockley–Queisser. In that case all recombination is supposed to be radiative [53–55]. It is worth mentioning that there are monomolecular trap-assisted recombination pathways that can predominate under normal solar cell operating conditions [45, 46].

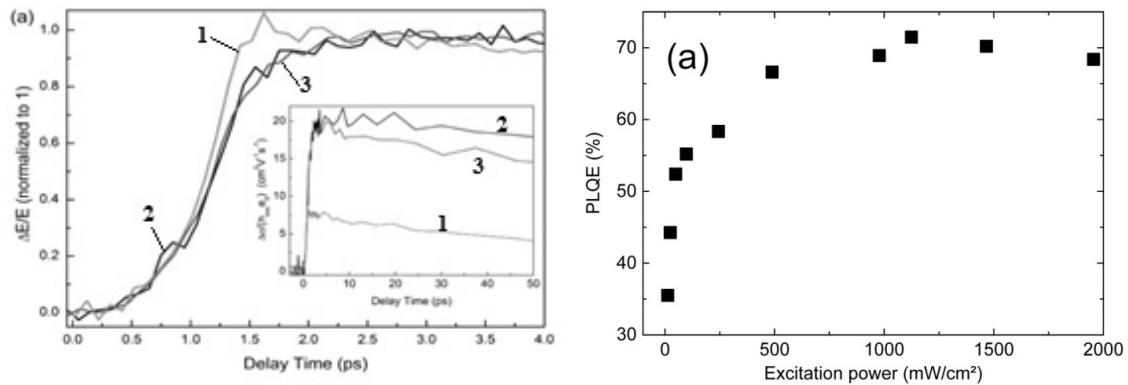


Figure 5. (a) Normalized early time terahertz dynamics of neat MAPbI₃ (2), MAPbI₃/mesoporous Al₂O₃ (3) and MAPbI₃/mesoporous TiO₂ (1) films following pulsed photoexcitation at 400 nm. Inset shows the THz photoconductivity kinetics for the first 50 ps normalized to give mobility values [49] (b) The photoluminescence quantum efficiency (PLQE) of a perovskite thin-film sample as a function of excitation power [48]

In case of planar heterojunction cells, it is known that the crucial prerequisite for proper operation of cell is that diffusion lengths of the electron and hole must be greater than the film thickness required to get entire solar light harvesting. The diffusion length has been estimated to be over 1 μm for both electrons and holes in films of MAPbI_{3-x}Cl_x (Fig. 5b) [36, 46]. This value is appropriately long for efficient operation of cell with planar heterojunction architecture as an absorption depth is approximately 400 nm at a wavelength of 700 nm [27, 33–36, 38, 56, 57]. The long diffusion length is explained by a long electron–hole lifetime of the order of 300 ns to microseconds [36].

Electron-beam induced current (EBIC) mapping technique has been used to determine operating principal of perovskite planar heterojunction solar cells (and mesosuperstructured solar cells). Result of EBIC revealed that their operating principal is similar to a thin-film *p-i-n* heterojunction solar cell [35, 37, 56, 58]. In EBIC scans (Fig. 6a, b), two peaks are observed that is consistent with *p-i-n* operation [37]. These results imply that most probable operating principle is that photon is absorbed and free charge carriers are generated at room temperature [45, 50, 52]. Further, generated charge carriers diffuse throughout the perovskite film and selectively move across their respective electrodes and where they promote the current in the external circuit [37].

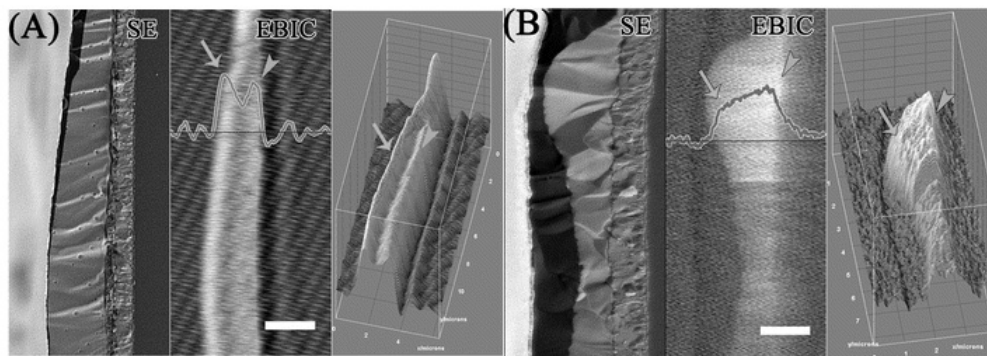


Figure 6. SE and EBIC images of cross sections of CH₃NH₃PbI_{3-x}Cl_x (A), scale bar is 2 μm , and CH₃NH₃PbI₃ (B), scale bar is 1 μm , planar solar cells. Line scans were taken at the lines' positions. The arrows show the peaks for the I–Cl and where the peaks are in the case of the pure iodide. The right panel is a 3D surface plot of the EBIC images. The ripples observed in the EBIC image of (A) outside the (semi-) conductive regions are due to background noise. Reprinted from [37]

The charge carrier diffusion lengths calculated by EBIC are approximately 2 μm for the I/Cl mixed halide perovskite and 1 μm for the hole diffusion in the triiodide perovskite. This result is in accordance with charge carrier diffusion lengths estimated for the two materials by terahertz time-domain spectroscopy [50], but longer than those estimated by time-resolved photoluminescence quenching measurements [36, 56].

Photoluminescence quenching measurements which will tend to give an underestimate due to the assumptions of perfect quenching and homogenous recombination throughout the bulk of the film.

The perovskite film morphology and the defect density within the films strongly influence on the charge carrier lifetime in the perovskite. According to recent research on single crystals of MAPbI₃ and MAPbBr₃, defect densities in such crystals are lower $\sim 10^{10} \text{ cm}^{-3}$ [59, 60], in comparison to the polycrystalline perovskite films where ones are $\sim 10^{16} \text{ cm}^{-3}$ [45, 46, 57]. In these single crystals, an estimated charge carrier lifetime and a corresponding charge carrier diffusion length reach value of a few hundred microseconds and of 175 μm , respectively. It is worth to mentioning that here to estimate the charge carrier lifetime electrochemical impedance spectroscopy and photovoltage decay techniques of electronically contacted crystals were used. If charge carrier trapping takes place at the crystal surface, it may overestimate the charge carrier lifetime, and in that case, the results require verification by other techniques.

In polycrystalline thin films, the intergrain potential barriers present obstacles to carrier transport through layer and may reduce the carrier mobility by many orders of magnitude from that found in single-crystal material. In this respect, CIGS has long been regarded a «better material» due to the extremely low intergrain potential barrier of 100 meV [58]. In comparison with CIGS, at the CdTe grain boundaries, depending on processing conditions, intergrain potential barrier is $\sim 100\text{--}800$ meV [58]. However, intergrain potential barrier in polycrystalline MAPbI₃ perovskite films in the dark is \sim only 45 meV, and further decreased under illumination [37]. This implies that charge trapping at grain boundaries in perovskite films must be much less of an obstacle than in CIGS or CdTe. However, cells with large grain size had enhanced device performance and charge carrier diffusion length which imply that the grain boundaries may not be benign [59, 60].

The steepness of the optical absorption edge indicates on the quality of the material. It allows to characterize the energetic disorder by analyzing the exponential decay of the absorption spectra below the bandgap with a characteristic energy, the Urbach energy [61, 62]. The perovskite films have a high absorption coefficient with a sharp absorption edge and a low Urbach energy of 15 meV, that means a low level of energetic disorder. For comparison, values of Urbach energy of GaAs, CdTe, crystalline silicon, MAPbI₃ or MAPbI_{3-x}Cl_x, CIGS are 7, 10, 11, 15, 25 meV, respectively. The Urbach energy of perovskite is lower than CIGS (~ 25 meV) and somewhat higher than GaAs (~ 7 meV) [54, 61], that is unbelievable for a solution prepared semiconductor. Despite that perovskite samples fabricated employing most standard solution-processing methods [45, 48, 51, 57] have low densities electronic trap states ($\sim 10^{16} \text{ cm}^{-3}$) in band gap, even the low trap states strongly influence on recombination dynamic [46], cell photovoltage [51], and photoluminescence quantum efficiencies [46, 48, 51] (Figure 6b).

In the most efficient perovskite solar cells using nanoporous TiO₂, the cell is composed of a thin (~ 200 nm) layer of nanoporous TiO₂ infiltrated and capped with a solid perovskite layer ($\sim 200\text{--}300$ nm) (Fig. 5a) [63–66]. In these nanoporous TiO₂-based perovskite cells, a bottom layer of TiO₂/perovskite perform a role of a bulk distributed heterojunction and a top layer of the perovskite and the hole-transport material operates as a planar heterojunction [63, 66]. Snaith et. al assume that as soon as proper control of the interfacial contact between the perovskite and the compact n-type layers is achieved, the privileged solar cell architecture will be the planar heterojunction one (Fig. 5b) [33, 37, 67].

3. Summary and perspectives

In summary, some major progresses on the development of perovskite based photocatalysts for water splitting have been achieved by following different modification strategies considering the fundamental principle and process of photocatalysis, crystal structure and chemical component characteristics of perovskite materials.

Intense research into perovskite solar cells and other optoelectronic applications has only recently begun, however a great breakthrough in solar cells has been made utilizing organolead halide perovskites as sunlight absorbers with low-cost preparation techniques. Organolead halide perovskites are capable of a high light harvesting, possess excellent electrotransport properties and have a low defect density and low intergrain potential barriers. PCEs of over 15 % have been reached for both mesoscopic architecture and planar heterojunction one. We believe that the increase in the domain size of crystals and the uniformity of perovskite film will be the major factors that will enhance the performance of perovskite solar cells over the next few years.

Acknowledgment

B.I gratefully acknowledges the Ministry of Education and Science of the Republic of Kazakhstan for the support of this work (program MSE Kazakhstan «NU-LBNL» 0115PK03029 and Grant no.535-F-15).

References

- 1 Nozik A.J. Photoelectrochemistry: Applications to Solar Energy Conversion // *Annu. Rev. Phys. Chem.* — 1978. — Vol. 29(1). — P. 189–222.
- 2 Lewis N.S. Powering the Planet // *MRS Bull.* — 2007. — Vol. 32. — P. 808–820.
- 3 Nocera D.G. Personalized Energy: The Home as a Solar Power Station and Solar Gas Station // *ChemSusChem.* — 2009. — Vol. 2(5). — P. 387–390.
- 4 Kojima A., Teshima K., Shirai Y., Miyasaka T. Organometal Halide Perovskites as Visible-Light Sensitizers for Photovoltaic Cells. // *J. Am. Chem. Soc.* — 2009. — Vol. 131(17). — P. 6050–6051.
- 5 Lee M.M., Teuscher J., Miyasaka T., Murakami T.N., Snaith H.J. Efficient hybrid solar cells based on meso-superstructured organometal halide perovskites // *Science.* — 2012. — Vol. 338. — P. 643–647.
- 6 Zhou H., Chen Q., Li G., Luo S., Song T.-B., Duan H.-S., Hong Z., You J., Liu Y., Yang Y. Interface engineering of highly efficient perovskite solar cells // *Science.* — 2014. — Vol. 345. — P. 542–546.
- 7 Kim H.S., Lee C.R., Im J.H., Lee K.B., Moehl T., Marchioro A., Moon S.J., Humphry-Baker R., Yum J.H., Moser J.E., Grätzel M., Park N.G. // *Sci. Rep.* — 2012. — Vol. 2. — P. 591.
- 8 Green M.A., Emery K., Hishikawa Y., Warta W., Dunlop E.D. // *Prog. Photovoltaics.* — 2014. — Vol. 22. — P. 701–710.
- 9 DeWolf S., Holovsky J., Moon S.-J., Lçper P., Niesen B., Ledinsky M., Haug F.-J., Yum J.-H., Ballif C. // *J. Phys. Chem. Lett.* — 2014. — Vol. 5. — P. 1035–1039.
- 10 Sadhanala A., Deschler F., Thomas T.H., Dutton S.E., Goedel K.C., Hanusch F.C., Lai M.L., Steiner U., Bein T., Docampo P., Cahen D., Friend R.H. // *J. Phys. Chem. Lett.* — 2014. — Vol. 5. — P. 2501–2505.
- 11 Stranks S.D., Eperon G.E., Grancini G., Menelaou C., Alcocer M.J., Leijtens T., Herz L. M., Petrozza A., Snaith H.J. // *Science.* — 2013. — Vol. 342. — P. 341–344.
- 12 Xing G., Mathews N., Sun S., Lim S.S., Lam Y.M., Grätzel M., Mhaisalkar S., Sum T.C. // *Science.* — 2013. — Vol. 342. — P. 344–347.
- 13 Wehrenfennig C., Eperon G.E., Johnston M.B., Snaith H.J., Herz L.M. // *Adv. Mater.* — 2014. — Vol. 26. — P. 1584–1589.
- 14 Edri E., Kirmayer S., Mukhopadhyay S., Gartsman K., Hodes G., Cahen D. // *Nat. Commun.* — 2014. — Vol. 5. — P. 3461.
- 15 Knittle E., Jeanloz R. Synthesis and Equation of State of (Mg, Fe)SiO₃ Perovskite to Over 100 Gigapascals // *Science.* — 1987. — Vol. 235(4789). — P. 668–670.
- 16 Cheng Z., Lin J. Layered organic-inorganic hybrid perovskites: structure, optical properties, film preparation, patterning and templating engineering // *Cryst. Eng. Comm.* — 2010. — Vol. 12(10). — P. 2646–2662.
- 17 Glazer A. The classification of tilted octahedra in perovskites // *Acta Crystallographica Section B.* — 1972. — Vol. 28(11). — P. 3384–3392.
- 18 Scaife D.E., Weller P.F., Fisher W.G. Crystal preparation and properties of cesium tin (II) trihalides // *J. Solid State Chem.* — 1974. — Vol. 9(3). — P. 308–314.
- 19 Li C. et al. Formability of ABX₃ (X= F, Cl, Br, I) Halide Perovskites // *Acta Crystallogr. Sect. B.* — 2008. — Vol. 64(6). — P. 702–707.
- 20 Umari P., Mosconi E., De Angelis F. Relativistic GW calculations on CH₃NH₃PbI₃ and CH₃NH₃SnI₃ perovskites for solar cell applications // *Sci. Rep.* — 2014. — Vol. 4. — P. 4467.
- 21 <http://news.sciencemag.org/2013/12/sciences-top-10-breakthroughs-2013>
- 22 Kojima A. et al. Organometal Halide Perovskites as Visible-Light Sensitizers for Photovoltaic Cells // *J. Am. Chem. Soc.* — 2009. — Vol. 131(17). — P. 6050–6051.
- 23 Kim H.-S. et al. High efficiency solid-state sensitized solar cell-based on submicrometer rutile TiO₂ nanorod and CH₃NH₃PbI₃ perovskite sensitizer // *Nano Lett.* — 2013. — Vol. 13. — P. 2412–2417.
- 24 Lee M.M., Teuscher J., Miyasaka T., Murakami T.N., Snaith Henry J. Efficient hybrid solar cells based on meso-superstructured organometal halide perovskites // *Science.* — 2012. — Vol. 338. — P. 643–647.
- 25 Heo J.H., Im S.H., Noh J.H., Mandal T.N., Lim C.S., Chang J.A., Lee Y.H., Kim H.J., Sarkar A., Nazeeruddin M.K., Grätzel M., Seok S.I. Efficient inorganic-organic hybrid heterojunction solar cells containing perovskite compound and polymeric hole conductors // *Nat. Photonics.* — 2013. — Vol. 7. — P. 487–492.
- 26 Burschka J., Pellet N., Moon S.J., Humphry-Baker R., Gao P., Nazeeruddin M.K., Grätzel M. Sequential deposition as a route to high-performance perovskite-sensitized solar cells // *Nature.* — 2013. — Vol. 499(7458). — P. 316–9.
- 27 Liu M., Johnston M.B., Snaith H.J. Efficient planar heterojunction perovskite solar cells by vapour deposition // *Nature.* — 2013. — Vol. 501. — P. 395–398.
- 28 Zhou H., Chen Q., Li G., Luo S., Song T.B., Duan H.S., Hong Z., You J., Liu Y., Yang Y. Photovoltaics. Interface engineering of highly efficient perovskite solar cells // *Science.* — 2014. — Vol. 345. — P. 542–546.
- 29 <http://www.nrel.gov>
- 30 Lee M.M., Teuscher J., Miyasaka T., Murakami T.N., Snaith H.J. Efficient Hybrid Solar Cells Based on Meso-Superstructured Organometal Halide Perovskites // *Science.* — 2012. — Vol. 338. — P. 643–647.

- 31 Ball J.M., Lee M.M., Hey A., Snaith H.J. Low-temperature processed meso-superstructured to thin-film perovskite solar cells // *Energy Environ. Sci.* — 2013. — Vol. 6. — P. 1739–1743.
- 32 Sun S., Salim T., Mathews N., Duchamp M., Boothroyd C., Xing G., Sum T.C., Lam Y.M. The origin of high efficiency in low-temperature solution-processable bilayer organometal halide hybrid solar cells // *Energy Environ. Sci.* — 2014. — Vol. 7. — P. 399–407.
- 33 Eperon G.E., Burlakov V.M., Docampo P., Goriely A., Snaith H.J. Morphological Control for High Performance Solution-Processed Planar Heterojunction Perovskite Solar Cells // *Advanced Functional Materials.* — 2014. — Vol. 24. — P. 151–157.
- 34 Dharani S., Mulmudi H.K., Yantara N., Thu Trang P.T., Park N.G., Graetzel M., Mhaisalkar S., Mathews N., Boix P.P. High efficiency electrospun TiO₂ nanofiber based hybrid organic–inorganic perovskite solar cell // *Nanoscale.* — 2014. — Vol. 6. — P. 1675–1679.
- 35 Liang K., Mitzi D.B., Prikas M.T. Synthesis and Characterization of Organic–Inorganic Perovskite Thin Films Prepared Using a Versatile Two-Step Dipping Technique // *Chem. Mater.* — 1998. — Vol. 10. — P. 403–411.
- 36 Chen Q. et al. Planar heterojunction perovskite solar cells via vapor-assisted solution process // *J. Am. Chem. Soc.* — 2014. — Vol. 136. — P. 622–625.
- 37 Malinkiewicz O. et al. Perovskite solar cells employing organic charge-transport layers // *Nature Photonics.* — 2014. — Vol. 8. — P. 128–132.
- 38 Snaith H.J., Schmidt-Mende L. Advances in liquid-electrolyte and solid-state dye-sensitized solar cells // *Adv. Mater.* — 2007. — Vol. 19. — P. 3187–3200.
- 39 Etgar L. et al. Mesoscopic CH₃NH₃PbI₃/TiO₂ Heterojunction Solar Cells // *J. Am. Chem. Soc.* — 2012. — Vol. 134. — P. 17396–17399.
- 40 Liu D., Kelly T.L. Perovskite Solar Cells with a Planar Heterojunction Structure Prepared using Room-Temperature Solution Processing Techniques // *Nature Photonics.* — 2014. — Vol. 8. — P. 133–138.
- 41 Stranks S.D. et al. Electron-hole diffusion lengths exceeding 1 micrometer in an organometal trihalide perovskite absorber // *Science.* — 2013. — Vol. 342. — P. 341–344.
- 42 Edri E. et al. Why lead methylammonium tri-iodide perovskite-based solar cells require a mesoporous electron transporting scaffold (but not necessarily a hole conductor) // *Nano Lett.* — 2014. — Vol. 14. — P. 1000–1004.
- 43 D'Innocenzo V. et al. Excitons versus free charges in organo-lead tri-halide perovskites // *Nature Commun.* — 2014. — Vol. 5. — P. 3586.
- 44 Even J., Pedesseau L., Katan C. Analysis of multivalley and multibandgap absorption and enhancement of free carriers related to exciton screening in hybrid perovskites // *J. Phys. Chem. C.* — 2014. — Vol. 118. — P. 11566–11572.
- 45 Saba M. et al. Correlated electron–hole plasma in organometal perovskites // *Nature Commun.* — 2014. — Vol. 5. — P. 5049.
- 46 Stranks S. D. et al. Recombination Kinetics in Organic-Inorganic Perovskites: Excitons, Free Charge, and Subgap States // *Phys. Rev. Appl.* — 2014. — Vol. 2. — P. 034007.
- 47 Stranks D. S., Snaith H.J. Metal-halide perovskites for photovoltaic and light-emitting devices // *Nature Nanotechnology.* — 2015. — Vol. 10. — P. 391–402.
- 48 Deschler F. et al. High Photoluminescence Efficiency and Optically Pumped Lasing in Solution-Processed Mixed Halide Perovskite Semiconductors // *J. Phys. Chem. Lett.* — 2014. — Vol. 5. — P. 1421–1426.
- 49 Ponseca C.S. Jr. et al. Organometal halide perovskite solar cell materials rationalized: Ultrafast charge generation, high and microsecond-long balanced mobilities, and slow recombination // *J. Am. Chem. Soc.* — 2014. — Vol. 136. — P. 5189–5192.
- 50 Wehrenfennig C., Eperon G.E., Johnston M.B., Snaith H.J., Herz L.M. High Charge Carrier Mobilities and Lifetimes in Organolead Trihalide Perovskites // *Adv. Mater.* — 2014. — Vol. 26. — P. 1584–1589.
- 51 Leijtens T. et al. Electronic Properties of Meso-Superstructured and Planar Organometal Halide Perovskite Films: Charge Trapping, Photodoping, and Carrier Mobility // *ACS Nano.* — 2014. — Vol. 8. — P. 7147–7155.
- 52 Manser J.S., Kamat P.V. Band filling with free charge carriers in organometal halide perovskites // *Nature Photon.* — 2014. — Vol. 8. — P. 737–743.
- 53 Tvingstedt K. et al. Radiative efficiency of lead iodide based perovskite solar cells // *Sci. Rep.* — 2014. — Vol. 4. — P. 6071.
- 54 Miller O.D., Yablonovitch E., Kurtz S.R. Strong Internal and External Luminescence as Solar Cells Approach the Shockley–Queisser Limit // *J. Photovoltaics.* — 2012. — Vol. 2. — P. 303–311.
- 55 Tress W. et al. Predicting the open-circuit voltage of CH₃NH₃PbI₃ perovskite solar cells using electroluminescence and photovoltaic quantum efficiency spectra: the role of radiative and non-radiative recombination // *Adv. Energy Mater.* — 2015. — Vol. 5. — P. 1400812.
- 56 Xing G. et al. Long-Range Balanced Electron and Hole-Transport Lengths in Organic-Inorganic CH₃NH₃PbI₃ // *Science.* — 2013. — Vol. 342. — P. 344–347.
- 57 Shao Y., Xiao Z., Bi C., Yuan Y., Huang J. Origin and elimination of photocurrent hysteresis by fullerene passivation in CH₃NH₃PbI₃ planar heterojunction solar cells // *Nature Commun.* — 2014. — Vol. 5. — P. 5784.
- 58 Edri E. et al. Elucidating the charge carrier separation and working mechanism of CH₃NH₃PbI_{3-x}Cl_x perovskite solar cells // *Nature Commun.* — 2014. — Vol. 5. — P. 3461.
- 59 Dong Q. et al. Electron-hole diffusion lengths >175 μm in solution-grown CH₃NH₃PbI₃ single crystals // *Science.* — 2015. — Vol. 347. — P. 967–970.
- 60 Shi D. et al. Low trap-state density and long carrier diffusion in organolead trihalide perovskite single crystals // *Science.* — 2015. — Vol. 347. — P. 519–522.
- 61 De Wolf S. et al. Organometallic Halide Perovskites: Sharp Optical Absorption Edge and Its Relation to Photovoltaic Performance // *J. Phys. Chem. Lett.* — 2014. — Vol. 5. — P. 1035–1039.
- 62 Sadhanala A. et al. Preparation of single-phase films of CH₃NH₃Pb(I_{1-x}Br_x)₃ with sharp optical band edges // *J. Phys. Chem. Lett.* — 2014. — Vol. 5. — P. 2501–2505.

- 63 Jeon N.J. et al. Compositional engineering of perovskite materials for high-performance solar cells // Nature. — 2015. — Vol. 517. — P. 476–480.
- 64 Heo J.H. et al. Efficient inorganic-organic hybrid heterojunction solar cells containing perovskite compound and polymeric hole conductors // Nature Photon. — 2013. — Vol. 7. — P. 486–491.
- 65 Leijtens T., Lauber B., Eperon G.E., Stranks S.D. and Snaith H.J. The importance of perovskite pore filling in organometal mixed halide sensitized TiO₂-based solar cells // J. Phys. Chem. Lett. — 2014. — Vol. 5. — P. 1096–1102.
- 66 Jeon N.J. et al. Solvent engineering for high-performance inorganic-organic hybrid perovskite solar cells // Nature Mater. — 2014. — Vol. 13. — P. 897–903.
- 67 Snaith H.J. Perovskites: The Emergence of a New Era for Low-Cost, High-Efficiency Solar Cells // J. Phys. Chem. Lett. — 2013. — Vol. 4. — P. 3623–3630.

Б.Р.Ильясов, Н.Х.Ибраев

Перовскитті күн ұяшықтарындағы жаңа жетістіктер

Мақалада гибриді (органикалық және бейорганикалық) перовскитті материалдар фотовольтаикада фотоактивті материалдар ретінде қолданылуы мүмкін. Қазіргі уақытта ғылыми-зерттеу топтарының жұмыстарының мақсаты кең оптикалық диапазонда жарық сәулесінің жұту қабілеттілігі жоғары перовскитті материалдардың дизайнын жобалауға бағытталған. $\text{CH}_3\text{NH}_3\text{PbX}_3$ (X — ионды галогендер қатарындағы) сияқты гибриді перовскиттер бірегей фотовольтаикалық және электрофизикалық қасиеттерді көрсете алады. Берілген жұмыстың басты мақсаты — күн батареяларында қолданылатын перовскитті наноматериалдар жайында соңғы жетістіктері жайлы ақпарат беріп, оларды әрі қарай дамыту жолдарын көрсету.

Б.Р.Ильясов, Н.Х.Ибраев

Новые достижения в перовскитных солнечных ячейках

В статье показано, что гибридные (органонеорганические) перовскитные материалы являются потенциальными фотоактивными материалами в фотовольтаике. Авторами отмечено, что в настоящее время много исследовательских групп сфокусированы на дизайне перовскитных материалов, способных поглощать солнечный свет в широком оптическом диапазоне. Гибридные перовскиты, такие как $\text{CH}_3\text{NH}_3\text{PbX}_3$ (X — ион из числа галогенов), демонстрируют уникальные фотовольтаические и электрические свойства. Выделена основная цель данной работы — показать последние достижения в области перовскитных наноматериалов, применяемых в солнечных батареях, и дать предпосылки для их дальнейшего улучшения.